An Evaluation of Multi-Component Weft-Knitted Twill Structures for Sensing Tensile Force – Supplement

Roland Aigner

May 2023

1 Introduction

This document represents supplementary material for the IEEE Sensors Journal article "An Evaluation of Multi-Component Weft-Knitted Twill Structures for Sensing Tensile Force" by Aigner and Hepper. The following chapters present more detail on some of the pre-evaluations and methods mentioned in the main paper, which were omitted there to avoid oververbosity.

2 Pre-evaluations

2.1 Correlation between width and height

As mentioned in the paper, in a preliminary evaluation we confirmed the results from [1], which found that sensor resistance is directly proportional to height and inversely proportional to width, with

$$R = \rho \frac{h}{w},$$

where ρ is a material-specific constant. Figure 1a illustrates this correlation; we varied the number of wales while keeping the number of courses constant, and vice versa. Resistance values were noted at idle (0 N) and strained (5 N) state respectively. Note that resistance values largely deviate from the ones in the main paper, since we knitted different sizes and furthermore used different materials, affecting ρ, however knitting structure was identical.

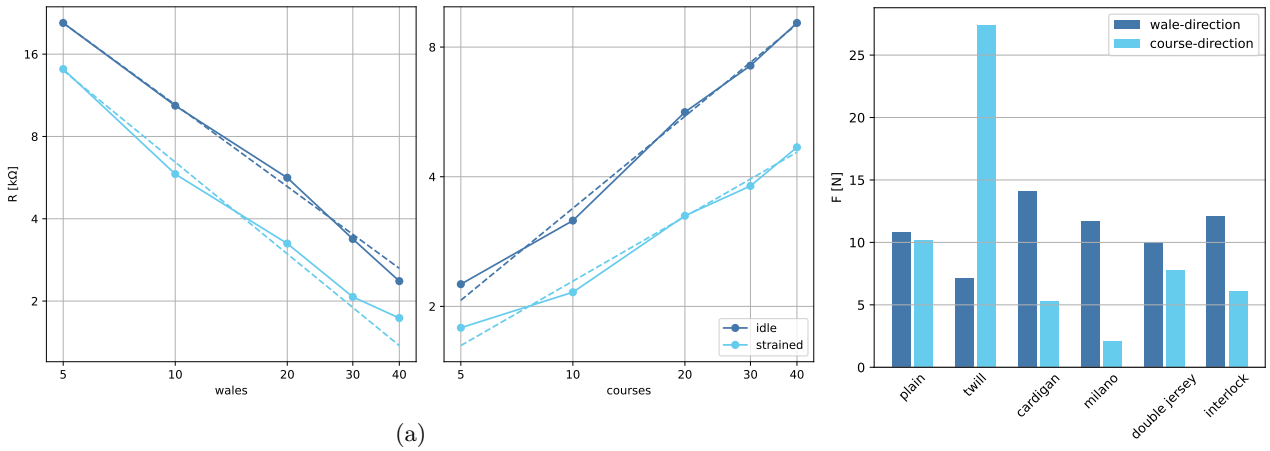

(a) (b)

Figure 1: (a) When the number of sensor wales (left) is changed, the sensor resistance changes proportionally. When the number of sensor courses (right) is changed, the resistance changes inversely proportional. (b) Twill, Cardigan, and Milano show highly anisotropic strain behavior. As a result of the structural composition, a Twill provides higher stability along course direction, while Cardigan and Milano provide higher stability along wale direction.

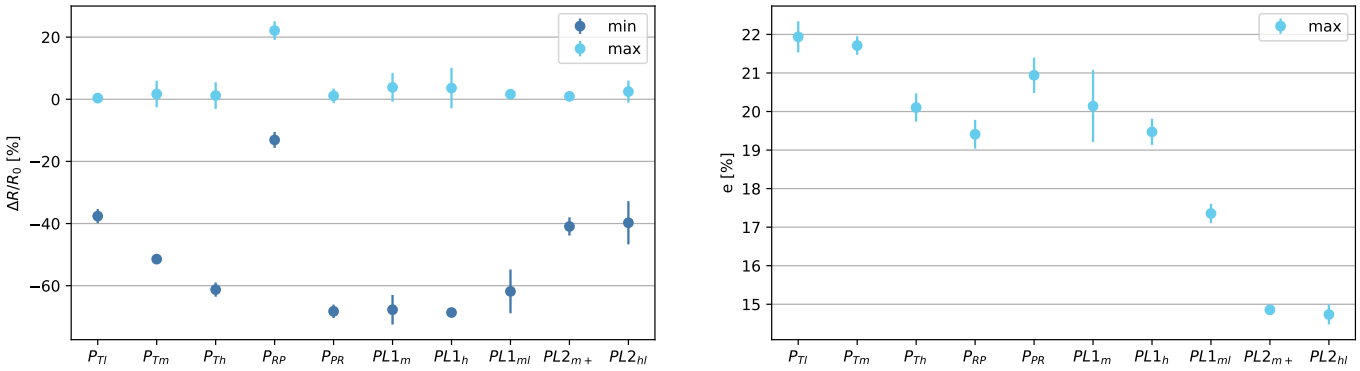

Figure 2: Mean values and SDs for sensor readings (left) and strain (right), when comparing sampling data from multiple sensor patches of the same type show reasonable within-sensor-design consistency.

2.2 Comparison of strain behavior of different knitting patterns

We furthermore evaluated strain behavior in an *ex-ante* evaluation. Using identical stitch settings and material, we knitted patches of 6 common patterns with equal sizes: Plain Knit (aka. Single Jersey), Twill, Cardigan, Milano, Double Jersey, Interlock. We then pulled each of those in our testing apparatus to a strain of e=40% along wale and along course direction and measured the required force. Figure 1b clearly shows that Twill, Cardigan, and Milano are highly anisotropic regarding straining behavior. In contrast to Milano and Cardigan, which provide better wale-directional stability due to the frequent tucks, a Twill shows the opposite behavior, which is a result of the high number of floats.

2.3 Sensor consistency

We knitted three samples of each of our sensor designs and therefore briefly investigated within-design consistency. We recorded data from repeated actuation using all of our sensor patches using our testing apparatus, stressing them repeatedly with 10 N, with our standard jog-rate. We removed the first actuation cycle as an outlier and we compared minima and maxima of $\Delta R/R_0$ out of the remaining data, as well as strain values e. Out of our 10×3 patches, we removed 2 outliers (one of type $\mathrm{P_{Tm}}$ and one of type $\mathrm{PL1_{ml}}$) that were showing fabrication related irregularities. Results from the remaining samples are presented in Figure 2, which shows satisfying standard deviations.

3 Long-term repetition

Next to long-term drift (see main paper), we tested our best-performing sensors for long-term behavior at repeated actuation. Using the standard jog rate of our testing apparatus, we repeatedly strained our sensors to e=20%, dwelling for 3 seconds after each movement (i.e., at e=0% and e=20%). We recorded 2,200 actuation cycles, which resulted in a testing duration of approx. 5.6 hours. Results can be seen in Figure 3. The main takeaway is that while settling behavior is similar, non-Lycra variants' dynamic range suffers most during this procedure.

4 Force-related data

For sake of comparability with related work, we presented plots in the main paper that are mostly related to strain. As mentioned however, our main motivation for this work was to sense *stress*, i.e., force. Hence, in Figure 4, we present timelines with relation to force. Furthermore, we show characteristics in Figure 5, including result of our course-directional tests of a sensor subset, as described in the main paper.

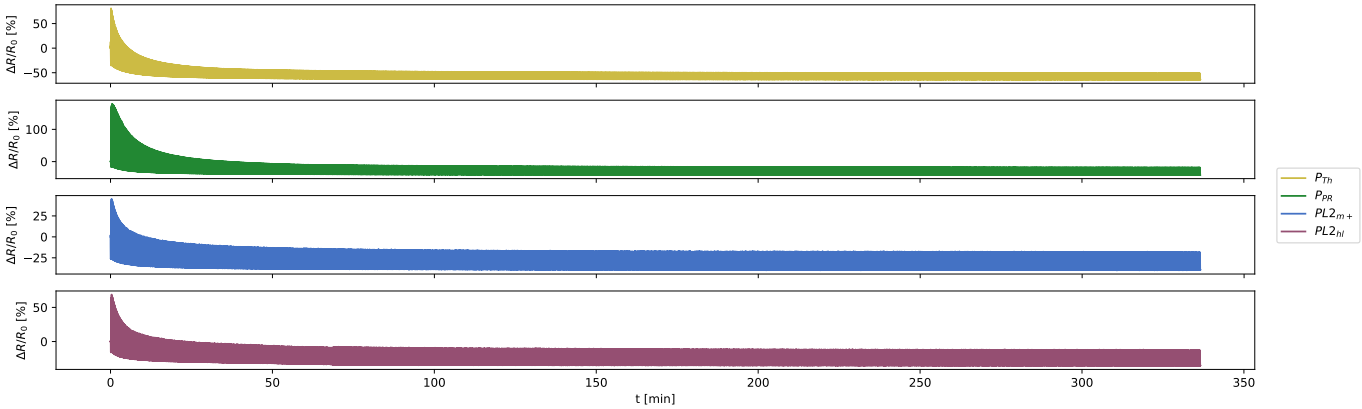

Figure 3: Long-term repeated actuation show that Lycra variants' dynamic range suffer least from constant actuation.

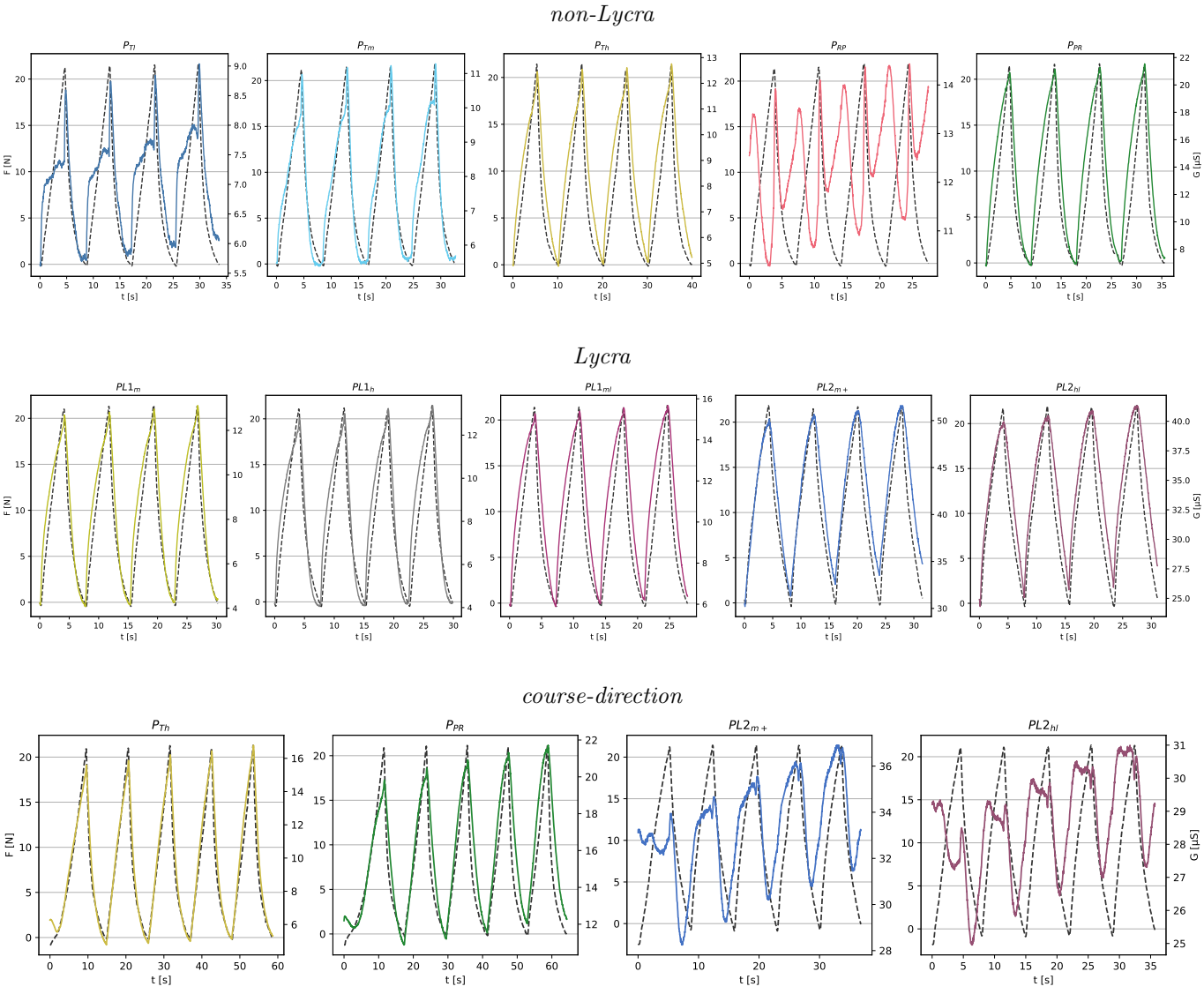

Figure 4: Timelines of non-Lycra (top) and Lycra (center) variants: overlaying force F (dashed, black) and sensor conductivity G, show respective conformity of our variations. Results of our tests actuating a sub-set along course-direction is presented at the bottom.

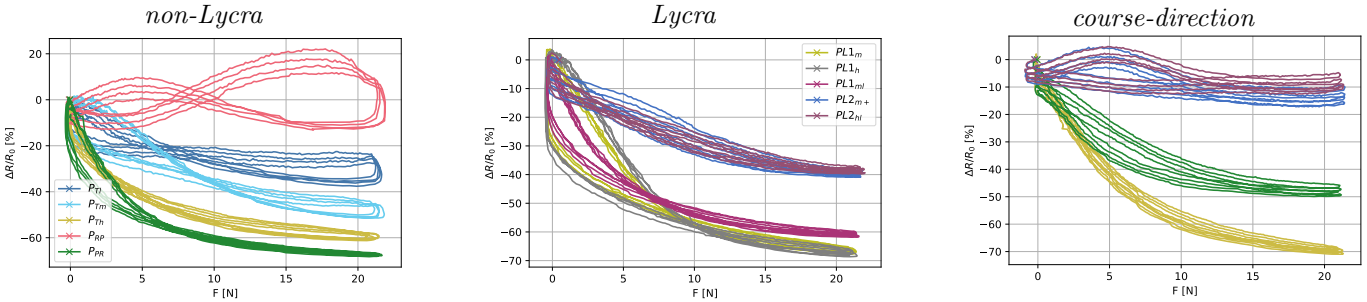

Figure 5: Plots of force F against relative resistance change $\Delta R/R_0$, showing characteristics of non-Lycra (left) and Lycra (center) variants, as well as results from course-directional actuation using a sub-set of our variations (right).

5 Details about line-fitting for calculation of hysteresis

To perform the line-fitting for calculating max. hysteresis, we first separated data into pulling and releasing segments. We noticed that most trends follow an exponential curve with constant offset, so we tried first to fit functions of type

$$y(x) = s \cdot 2^{a(x+o)} + d\,,$$

using SciPy function `optimize.curve_fit`[1] however, we noticed that the best fits were still off by a linear function, so we added another linear term $k \cdot x$ to get

$$y(x) = s \cdot 2^{a(x+o)} + k \cdot x + d\,.$$

The resulting fit curves can be seen in Figure 6 and the respective parameters can be found in Table 1, along with corresponding r^2 values. Since F/R characteristics were highly erratic for $\mathrm{P_{RP}}$, we excluded this set. We repeated the same for course-directional pulling, however only for $\mathrm{P_{Th}}$ and $\mathrm{P_{PR}}$, since Lycra-variants PL* were again not performing well (see main paper); the result can be seen in Figure 7, parameters are found in Table 2.

We calculate hysteresis with the absolute difference between the fit curves. Furthermore, we plot difference of binned data samples. Samples were therefore split the data samples into 100 bins that were equally distributed along the x-axis (F) and calculated mean values for each bin. We did this for pull- and release samples separately and calculated absolute difference, which is plotted as "binned diff" in Figures 6 and 7.

[1] `https://docs.scipy.org/doc/scipy/reference/generated/scipy.optimize.curve_fit.html`

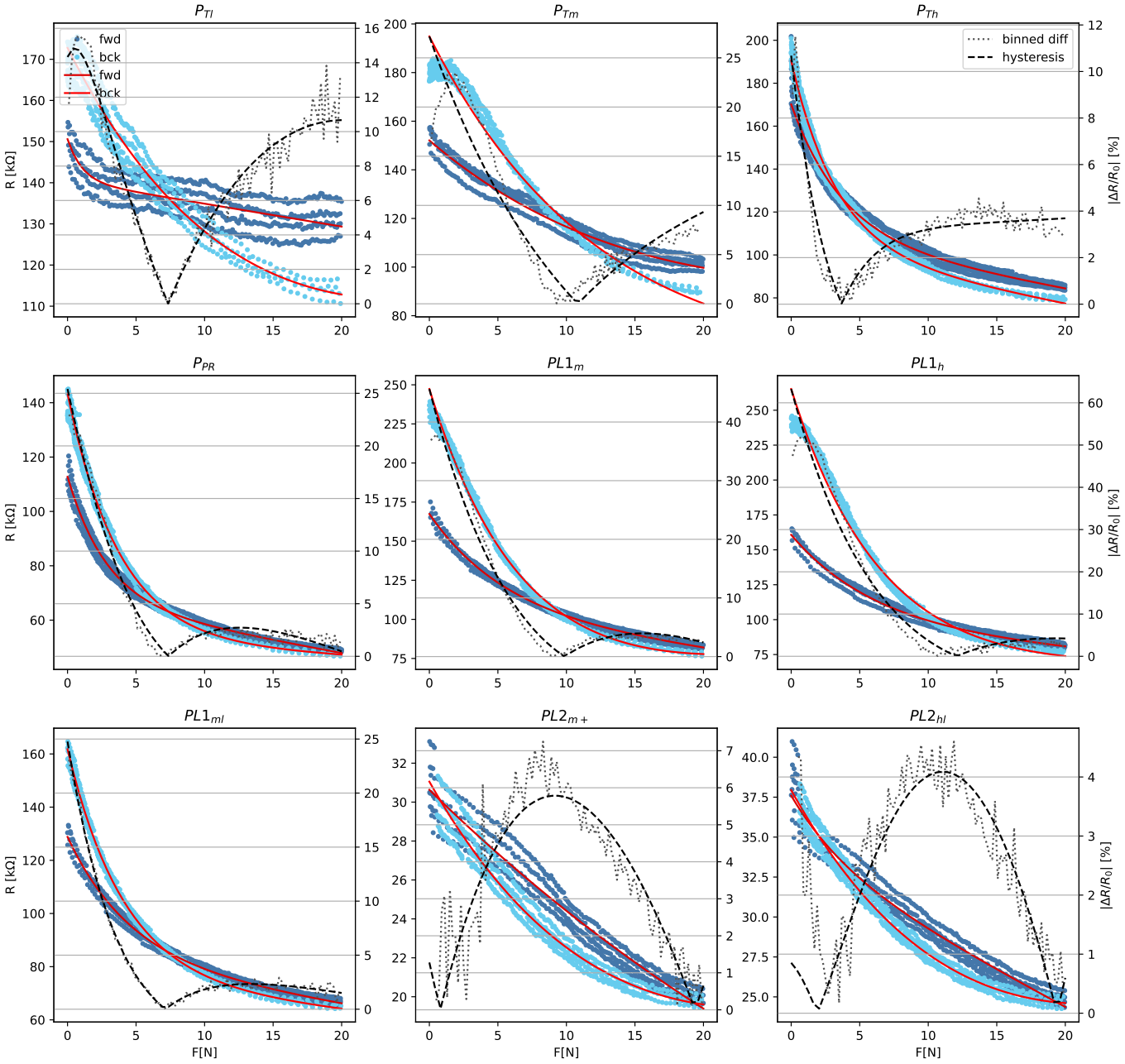

Figure 6: Lines fit to pulling and releasing segments of captured samples for wale-directional ("vertical") testing. Hysteresis in the paper is reported based to the fit curves.

Table 1: Parameters of fitted curves for wale-directional testing, as determined using `curve_fit`.

		a	s	d	k	o	r^2
P_{tl}	pull	-1.35	15.8	140	-0.556	0.479	0.570
	release	-0.0897	100	36.3	1.86	-5.00	0.952
P_{tm}	pull	-0.0696	100	24.8	1.32	-5.00	0.958
	release	-0.112	100	47.6	0.302	-5.00	0.959
P_{th}	pull	-0.386	36.5	108	-1.17	-2.02	0.982
	release	-0.436	43.1	102	-1.26	-2.36	0.988
P_{pr}	pull	-0.507	26.8	66.5	-0.935	-1.55	0.989
	release	-0.381	45.3	52.0	-0.257	-2.65	0.993
$PL1_{m}$	pull	-0.260	38.7	103	-1.14	-2.81	0.991
	release	-0.210	100	40.5	1.30	-5.00	0.992
$PL1_{h}$	pull	-0.233	38.8	93.8	-0.778	-3.38	0.982
	release	-0.217	100	53.2	0.509	-5.00	0.983
$PL1_{ml}$	pull	-0.317	28.0	82.3	-0.835	-2.31	0.990
	release	-0.347	42.3	74.2	-0.532	-3.02	0.996
$PL2_{m+}$	pull	-0.0317	27.4	2.61e-08	-0.0178	-5.00	0.956
	release	-0.0797	23.6	7.66e-10	0.466	-5.00	0.962
$PL2_{hl}$	pull	-0.349	3.68	33.5	-0.458	-0.450	0.964
	release	-0.08264	28.5	2.18e-05	0.627	-5.00	0.983

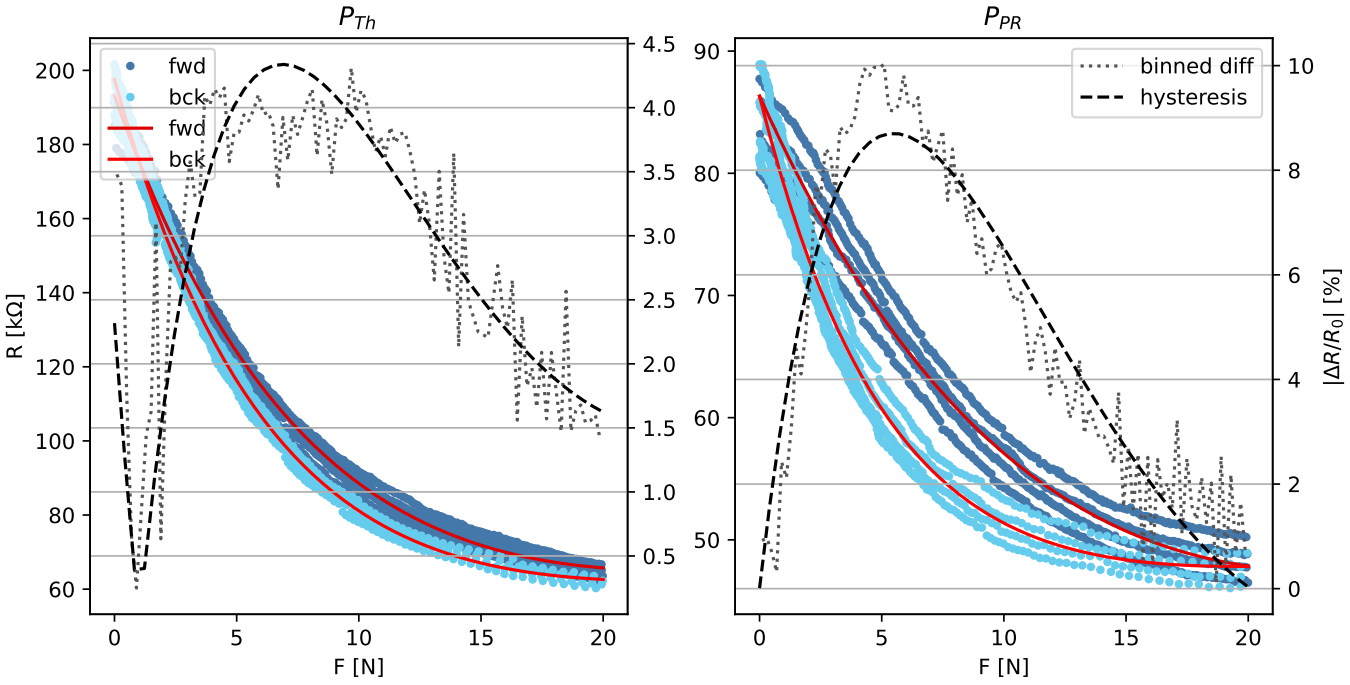

Figure 7: Lines fit to pulling and releasing segments of captured samples for course-directional ("horizontal") testing. Hysteresis in the paper is reported based to the fit curves.

Table 2: Parameters of fitted curves for course-directional testing, as determined using `curve_fit`.

		a	s	d	k	o	r^2
P_{th}	pull	-0.167	97.6	19.0	1.47	-5.0	0.993
	release	-0.225	77.0	40.9	0.743	-4.54	0.993
P_{pr}	pull	-0.0947	62.2	5.40-15	1.23	-5.0	0.968
	release	-0.271	27.5	42.6	0.212	-2.46	0.969

References

[1] J. Ou, D. Oran, D. D. Haddad, J. Paradiso, and H. Ishii, "Sensorknit: Architecting textile sensors with machine knitting," *3D Printing and Additive Manufacturing*, vol. 6, no. 1, pp. 1–11, 2019. [Online]. Available: https://doi.org/10.1089/3dp.2018.0122